

Adaptive Position Calibration Technique for an Optical Micro-scanning Thermal Microscope Imaging System

BoZhi Zhang¹, MeiJing Gao^{1,2*}, Paul L. Rosin², Xianfang Sun², QiuYue Chang¹,
ChunYang Peng¹, QiChong Yan¹, Pan Chen¹, Yucheng Shang¹

(1. The Key Laboratory for Special Fiber and Fiber Sensor of Hebei Province, School of Information Science and Engineering, Yanshan University, Qinhuangdao, Hebei 066004, China

2. School of Computer Science and Informatics, Cardiff University, UK)

Abstract: In order to improve the spatial resolution of an optical micro-scanning thermal microscope system, the micro-scanning position must be accurately calibrated. An adaptive calibration method based on image registration and plane coordinate system is proposed. The meaning of calibration is given, and the principle and method of point calibration are introduced in detail and experiments using the real system were done. Different reconstruction methods were applied to reconstruct the visible light image and the real thermal microscope image, and the evaluation scores are given. Results of simulation and real thermal imaging processing show that the method can successfully calibrate the micro-scanning position. The method can significantly improve the oversampled reconstructed image quality, thus enhancing the system's spatial resolution. This method can also be used in other electro-optical imaging systems.

Keywords: optical micro-scanning; thermal microscope imaging system; image registration; adaptive position calibration

1 Introduction

Any object that is above absolute zero degrees will radiate energy outwards in the form of electromagnetic waves. Because infrared thermal imaging systems are temperature-sensitive, they can not only image the target, but also indicate the change of the target's temperature, and have been widely used in the military and civil fields^[1-4]. Thermal microscope imaging systems can monitor the shape and temperature of small objects, and so have been applied in the fields of nanotechnology, biochemical technology, genetic technology, microelectronics technology, and materials science^[5-6]. Because the focal plane array has few pixels, large unit pixel size, and low sampling frequency, thermal microscope imaging systems are under-sampled, which can easily cause image aliasing^[7-9]. Micro-scanning technology can be applied to improve imaging quality. The micro-scanning technology controls the movement of the optical

device using a mechanical device, so that the acquired images contain micro-displacements to obtain micro-scanning images, from which higher resolution images can be obtained. The technology uses a micro-scanning device to form an image of an infrared optical system into a $1/N$ (N is an integer) pixel distance in the x, y -direction, and obtains $N \times N$ frame under-sampled images. Then the multiple frame sub-pixel displaced images are reconstructed into one frame by using digital image processing technology. The number of pixels in the image is N^2 times that of the original image, so that more scene information can be obtained and the spatial resolution of the system can be improved from the lower resolution image provide by the detector^[10-12]. We have studied and built a high-resolution thermal microscope imaging system based on an in-plane rotation micro-scanner, as shown in Fig.1. Since the optical micro-scanning thermal microscope imaging system is a detachable device, the positional relationship between the detector and the micro-scanner will change after each adjustment, and calibration of the point position of the 2×2 micro-scan is required. Therefore, reference [13] proposed a zero calibration method, which calibrates the initial position, and then rotates the optical plate in steps of 90° to find the other three micro-scan position points. However, we redesigned the system and there were limitations of machining precision, and so the initial point (zero point) and the other three standard points which are only calibrated by the zero calibration method will have errors. Then, the actual step size of the system and the ideal step size of the design also have errors. The accumulation of errors caused the quadrilateral formed by the four micro-scanning positions in the experiment to deviate from the square formed by the standard micro-scanning, resulting in an undesirable effect. Therefore, calibration of the micro-scanning position for the system is a problem that needs to be solved at present. This paper proposes a calibration technique which is based on an image registration and plane coordinate system^[14-15].

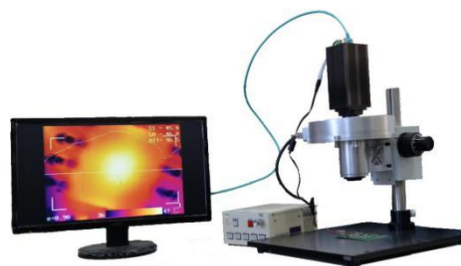


Fig.1 Optical micro-scanning thermal microscope imaging system

The paper is organized as follows. In Section 2, we introduce the structural composition of the micro-scanning thermal microscope imaging system and the working principle of the micro-scanning device. In Section 3, we propose an adaptive point calibration method. The calibration methods for the horizontal and vertical adjacent position points and diagonal position points are analyzed, and the adaptive

calibration process is introduced in detail. In Section 4, we verify the effectiveness of the adaptive calibration method for each point through the actual system position calibration experiment, the infrared image simulation experiment and the actual acquisition thermal microscope image reconstruction experiment. In Section 5, we summarize the paper and list the advantages of our proposed technique.

2 System composition and the working principle of the micro-scanning device

The optical micro-scanning thermal microscope imaging system consists of a thermal imaging component, a micro-scanner, an infrared microscope, an image acquisition card, an image processing system, a mount for the optical plate, and a power supply^[12]. Fig.2 shows the block diagram of the optical micro-scanning thermal microscope imaging system.

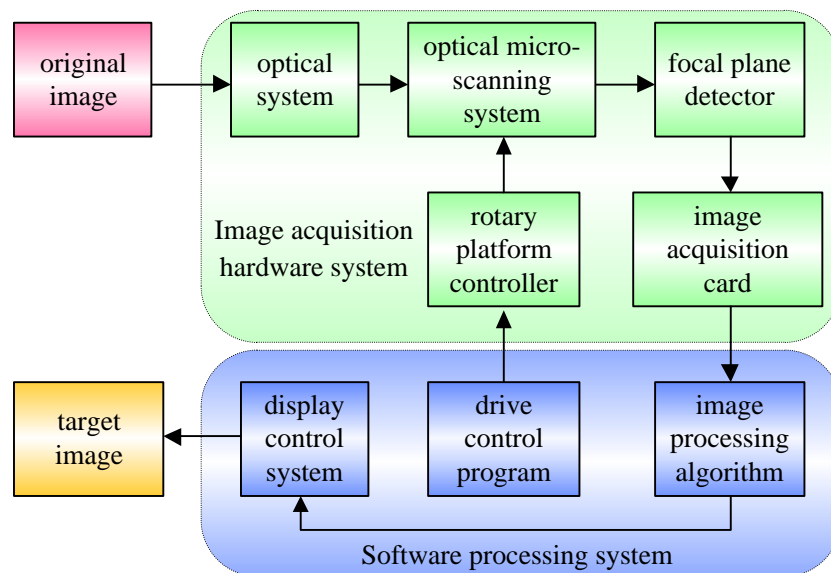


Fig.2 Block diagram of optical micro-scanning thermal microscope imaging system

Fig.3 shows an optical flat-rotation micro-scanning device containing an optical plate having a certain inclination angle of the optical axis. The optical flat-rotation micro-scanning device is located between the objective optical lens and the detector, and the mechanical device controls the rotation of the optical plate refractive lens around the optical axis. We collected four images at intervals of 90° from the standard micro-scanning position zero so that the four images are offset from each other by $9/2$ detector pitch, and finally, the super resolution image is obtained by oversampling reconstruction^[13].

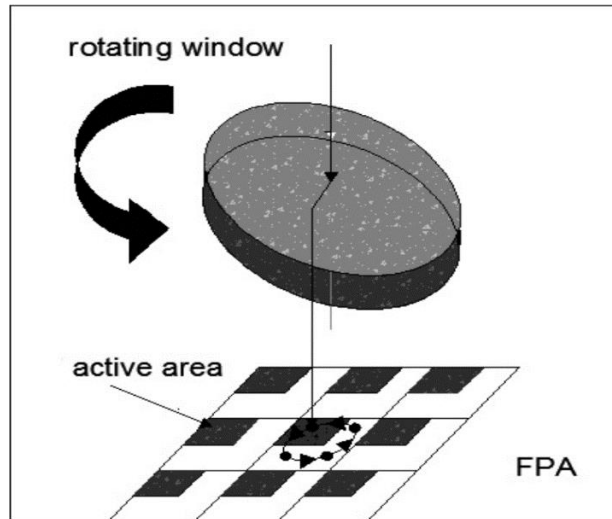


Fig.3 Schematic diagram of micro-scanning rotating refractor

When the optical plate rotates, the focus point of the concentrated beam will form a circle on the focal plane detector with the optical axis as the center and Δ as the radius. If the rectangular coordinate system of the detector array is used as the reference, the four positions on the circumference at 45° , 135° , 225° , and 315° are the micro-scan standard position points, and the four positions constitute a standard square, as shown in Fig.4. The distance between each pair of adjacent scanning positions is $9/2$ times the detector pixel spacing L , and its equivalent relationship is $\sqrt{2}\Delta=9L/2$. Four low-resolution under-sampled images are acquired at the standard position and reconstructed to obtain a single high-quality super resolution image^[16].

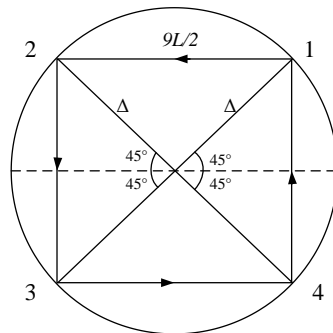


Fig.4 Standard micro-scan position map

Since the thermal imaging component of the system is a detachable mode, the relative position of the optical plate and micro-scanner changes after each reinstallation. If the scanning is still performed according to the previously determined rotational position, due to the deviation of the micro-scan zero position, the four micro-scanning positions are not formed into an ideal square.

We have completed the calibration of the micro-scan zero position in the early stage. As shown in Fig.5, the micro-displacement map after zero calibration (blue line)

is closer to the standard square (black line) than the uncalibrated micro-displacement map (red line). However, due to hardware limitations, the actual micro-scan step size of the system will have errors. Even if the initial position coincides with the standard position, the points at other positions still have errors for the standard position points. Therefore, the calibration of the micro-scan zero point position and the subsequent calibration of each scanning position are necessary [17].

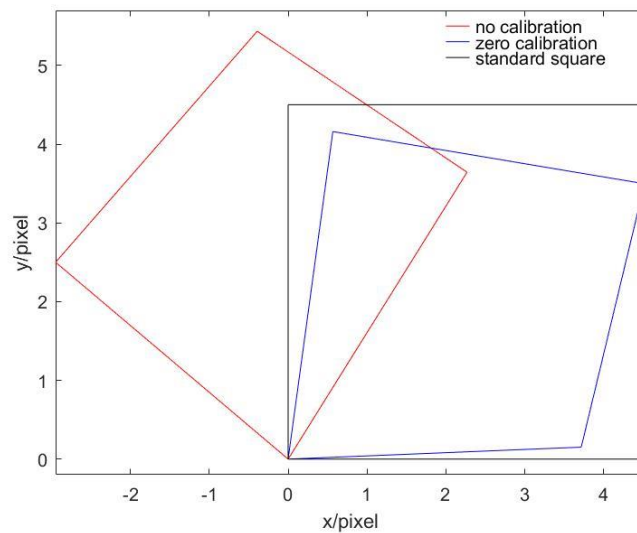


Fig.5 Zero calibration experiment of system micro-scanning position

3 Calibration of micro-scanning position of the micro-scanning device

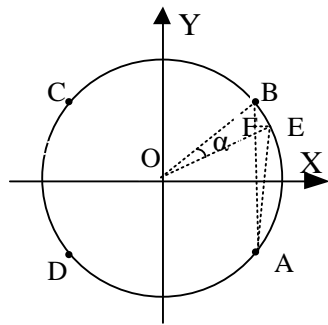
The calibration of the micro-scanning position means that all three micro-scanning position points, except the zero point, are accurately calibrated. Based on the geometric method and the improved frequency domain registration method [18], we calculate the related micro-displacements of the images to get the rotation angle and rotation direction with which we can determine the position of the standard point. By calibrating the adjacent position points and the diagonal position points, the remaining three micro-scanning points are finally accurately calibrated, thus further improving the spatial resolution of the system.

3.1 Adjacent position point calibration

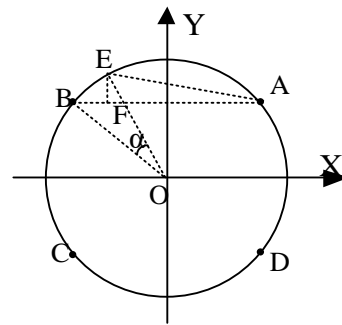
The optical plate is rotated 90° counterclockwise from the zero position to find its adjacent position. As shown in Fig.6(a), taking point A as the scanning zero-point as an example, rotating the plate refractor 90° counterclockwise should theoretically reach the standard position point B, but due to deviations in the system, it may fall at point E (x_E, y_E) . In order to calculate the value of α , draw the line segment EF through point E and make it perpendicular to AB. Connect AE, EO, BO. The size of the calibration angle α is equal to the size of $\angle BOE$. $\angle BOE$ and $\angle BAE$ are the central and

circumferential angles corresponding to the arc BE. Let Δx and Δy represent the difference between the horizontal and vertical coordinates of the two points A and E, then the size of the calibration angle α of the adjacent points is:

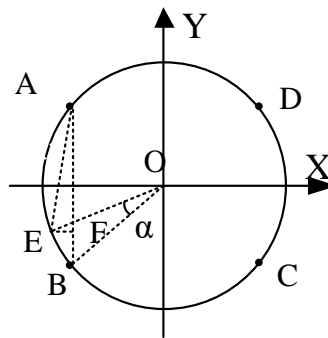
$$\alpha = 2 \arctan \left| \frac{\min(\Delta x, \Delta y)}{\max(\Delta x, \Delta y)} \right| \times \text{sgn}(\Delta x \times \Delta y) \quad (1)$$



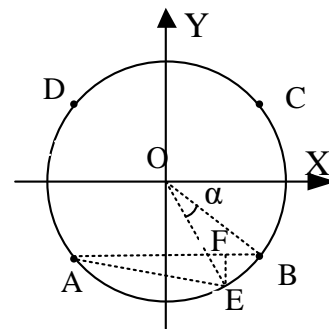
(a) Calibration point in the first quadrant



(b) Calibration point in the second quadrant



(c) Calibration point in the third quadrant



(d) Calibration point in the fourth quadrant

Fig.6 Adjacent position calibration diagram

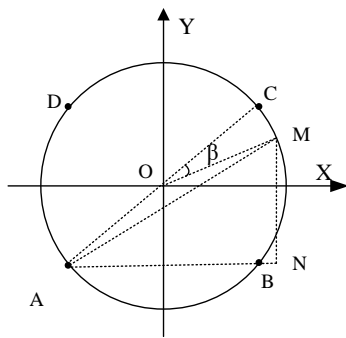
When the point to be calibrated is in other quadrants, the method of calculating the calibration angle α is the same as in the case of the first quadrant. The direction of rotation of the optical plate will be discussed below. As can be seen from Fig.6, the direction of rotation of the micro-scanning device is related to the quadrant of the point to be calibrated: When the point to be calibrated is in the first and third quadrants, if $\alpha > 0$, the optical plate needs to be rotated counterclockwise by $|\alpha|$; when $\alpha < 0$, the optical plate needs to be rotated clockwise $|\alpha|$. When the point to be calibrated is in the second and fourth quadrants, if $\alpha > 0$, the plate refractor needs to be rotated clockwise $|\alpha|$, and when $\alpha < 0$, the plate refractor needs to be rotated counterclockwise $|\alpha|$.

3.2 Diagonal position point calibration

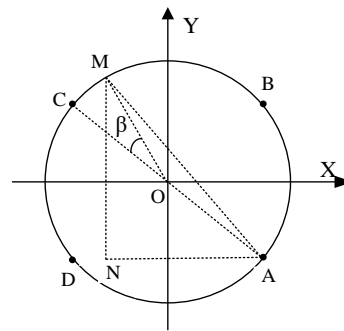
After completing the calibration of the point adjacent to the zero point, continue

to rotate the optical plate 180° to find its diagonal position point. As shown in Fig.7(a), take the point to be calibrated in the first quadrant as an example. After rotating the optical plate by 180° , it is challenging to align it precisely at the standard position. In theory, it should reach point B but falls at point $M(x_M, y_M)$. In order to find the value of β , draw a line segment MN through point N and make it perpendicular to AB. Connect, MO, AM, AC. The size of the calibration angle β is equal to the size of $\angle COM$. $\angle COM$ and $\angle CAM$ are the central and circumferential angles corresponding to the arc CM, Let Δx and Δy represent the difference between the horizontal and vertical coordinates of the two points A and M, then the size of the calibration angle β of the diagonal position point is:

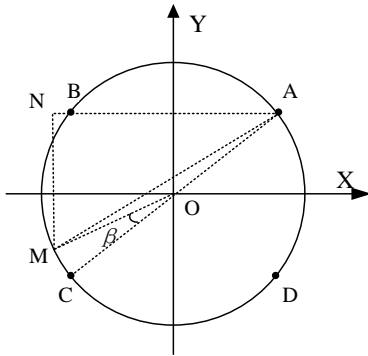
$$\beta = 2(45^\circ - \arctan \left| \frac{\Delta y}{\Delta x} \right|) \quad (2)$$



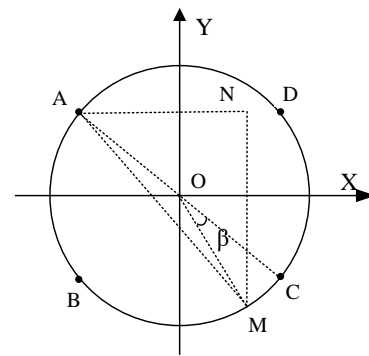
(a) Calibration point in the first quadrant



(b) Calibration point in the second quadrant



(c) Calibration point in the third quadrant



(d) Calibration point in the fourth quadrant

Fig.7 Diagonal position calibration diagram

When the point to be calibrated is in other quadrants, the method of calculating the calibration angle β is the same as in the case of the first quadrant. We know that the rotation direction of the optical plate is related to the quadrant of the point to be calibrated and the sign of β . When the point to be calibrated is in the first and third quadrants, if $\beta < 0$, the optical plate needs to be rotated clockwise by $|\beta|$; when $\beta > 0$, the

optical plate needs to be rotated counterclockwise $|\beta|$. When the point to be calibrated is in the second and fourth quadrants, if $\beta > 0$, the plate refractor needs to be rotated clockwise $|\beta|$, and when $\beta < 0$, the plate refractor needs to be rotated counterclockwise $|\beta|$.

3.3 Adaptive position calibration process

After calibrating two points according to the above method, starting from the third point, the optical plate is rotated clockwise by 90° , and the fourth point is calibrated according to the calibration method of the adjacent position point.

Due to hardware limitations, the position after one calibration will deviate from the ideal position. In the process of calibrating each point, each point is repeatedly calibrated until the angle threshold is satisfied. The threshold should be small in order that we do not need to repeat too many iterations. After many experiments, the threshold selected in this experiment is 1.5° . The adaptive calibration process of each position point is: firstly, an image I_1 is collected from the micro-scan zero point, and then the optical plate is rotated 90° to collect the image I_2 . We calculate the micro-displacement between the image I_1 and the image I_2 with the image registration algorithm. We calculate the calibration angle and the rotation direction according to the proposed adaptive calibration method and compare the calibration angle with the set threshold. If the calibration angle is greater than the threshold, rotate the plate to the new position according to the calculated calibration angle and rotation direction, re-acquire the image I_2 at the position, and then repeat the above process to obtain a new calibration angle and rotation direction. Otherwise, the adaptive position calibration is completed, and the calibration of the next position point is performed. The calibration flow chart is shown in Fig.8. This method of adaptive position calibration can improve the calibration accuracy and make the micro-scanning position of each point more accurate.

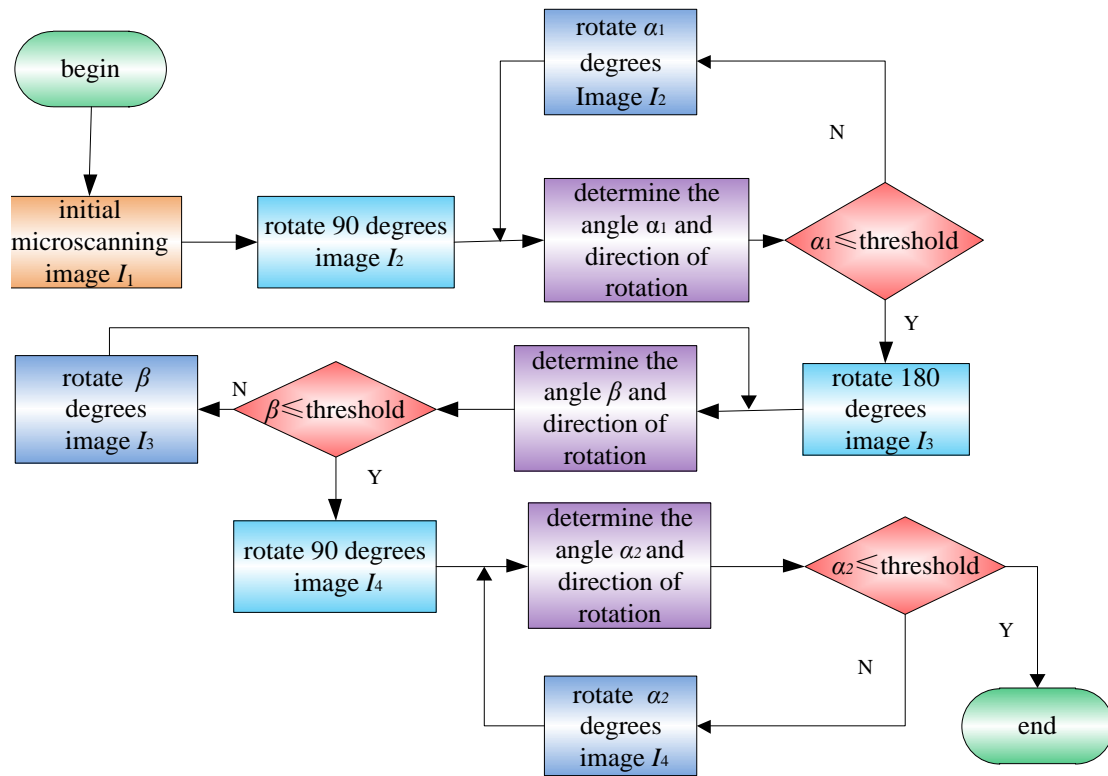


Fig.8 Flow chart of adaptive-position calibration

4 Position calibration and image reconstruction experiment

4.1 Actual system position calibration experiment

The calibration experiments of each point were performed for the micro-scanning thermal microscope imaging system with the proposed technology. Fig.9 is the displacement map of the four sets of experiments, showing the comparison of the micro-displacement position maps of the four images before and after the calibration of the scanning position. The red line in the figure indicates the micro-displacement diagram of the four images acquired at every 90° position from the mechanical zero-point without calibration. The blue line represents the micro-displacement map of the four images obtained by every 90° from the zero point with the calibration of the zero point. The green line indicates the micro-displacement map of the four images collected every 90° degrees starting from the micro-scan zero point after the calibration of each point is completed. The black line indicates the micro-displacement map of the four images obtained by the standard 2×2 micro-scanning.

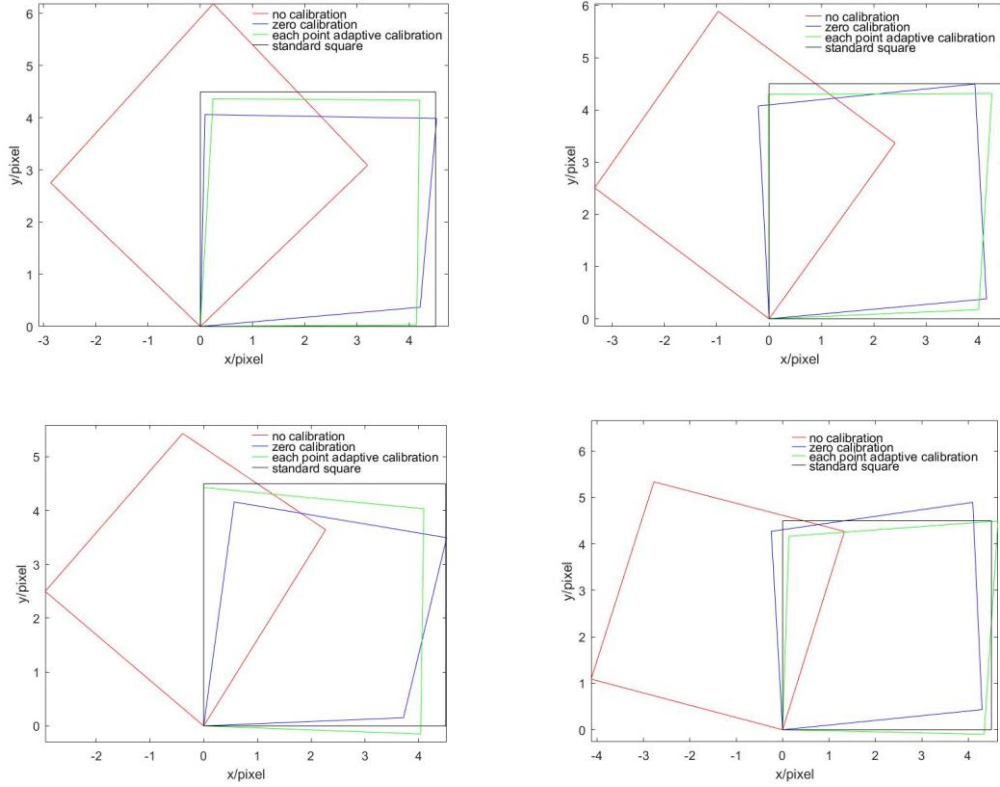


Fig.9 Micro-scanning position calibration experiment for thermal microscope system

It can be seen from Fig.9 that the position map of the four images acquired by the system without calibration substantially deviates from the ideal square which is the standard 2×2 micro-scanning position map, and the displacement map with the zero position calibration is improved relative to the uncalibrated displacement map. However, there is still a large offset compared with the standard position point. The micro-displacement position map when each point is adaptively calibrated is closer to the standard ideal square, and each micro-scanning position is closer to the standard micro-scanning position. The reconstructed image under this micro-displacement also theoretically has a higher resolution. Next, the oversampling reconstruction experiments are carried out according to the micro-displacement of the four images in three cases (zero calibration, adaptive point calibration, no calibration), which further proves the effectiveness of the calibration technology proposed in this paper.

4.2 Simulation Experiment of Lena image

According to the coordinates after adaptive calibration of each point, Fig.10(a) is down-sampled to generate four low-resolution images (as shown in Fig.10(b)), and Fig.10(b) is constructed to obtain Fig.11(c) with the oversampling reconstruction method in accordance with standard 2×2 micro-scanning. According to the coordinates after zero calibration, Fig.10(a) is down-sampled to generate four low-resolution

images, the same reconstruction method is applied to obtain the high-resolution image shown in Fig.11(b). Similarly, according to the uncalibrated coordinates, the reconstruction method is applied to obtain Fig.11(a).



(a) High-resolution image (b) Low-resolution images of simulation displacement
 Fig.10 High-resolution image and low-resolution images of simulation displacement



a) No calibration b) Zero calibration c) Adaptive point calibration

Fig.11 Simulation of oversampled reconstruction thermal images

As shown in Fig.11, the oversampled reconstructed image (no calibration) has more jaggies, and the details are not clear. The oversampled reconstructed image with zero calibration has more details and less jaggies, but some details are blurred. The oversampled reconstructed image after calibration (adaptive point calibration) has sharper textures and details and higher spatial resolution.

We performed four sets of repeated experiments and selected the following scores such as information entropy (H), peak signal-to-noise ratio (PSNR), and structural similarity index (SSIM)^[19] to evaluate the quality of reconstructed images^[20-22]. Table 1 gives the average evaluation scores of the simulation results. In order to compare different calibration methods better, this paper also selects the bilinear interpolation method for comparison.

Table 1 Evaluation scores of Lena image reconstruction

Image processing methods	H	PSNR	SSIM
Bilinear interpolation	7.3919	70.9967	0.7231
Oversample (no calibration)	7.4097	74.8601	0.8433
Oversample (zero calibration)	7.4189	76.7889	0.9118
Oversample (adaptive point calibration)	7.4206	76.8527	0.9139

PSNR is an objective measure of image distortion or noise level. A more substantial PSNR value indicates less distortion; SSIM is a measure of the similarity of two images. The closer the SSIM value is to 1, the better the similarity between the two images. H is an important parameter to measure the richness of image information. The larger the H value, the richer the information contained in the image. Comparing the average value of the evaluation scores PSNR, it can be found that the detail resolution ability (facial features and facial contour, hairline, etc.) of the oversampled reconstructed image after calibration (adaptive point calibration) is better than the other three methods (bilinear interpolation, zero calibration and no calibration). Comparing the average value of the evaluation scores SSIM and H, it can be found that the oversampled reconstructed images after calibration (adaptive point calibration) have higher similarity and richer details. The proposed technology improves the image information, which increases the image's resolvable details; in particular the image quality of the reconstructed image is greatly improved compared with the uncalibrated reconstruction and bilinear interpolation. Therefore, the proposed adaptive calibration technology for each point is effective.

4.3 Reconstruction experiment for thermal microscope images

As shown in Fig.12, after adaptive position calibration of each point was made, four low-resolution images of individual coins were collected from the optical micro-scanning thermal microscope imaging system. We combine the four low-resolution images to obtain the high-resolution image shown in Fig.13(a). Fig.13(b) is an oversampled reconstructed image obtained by performing only zero calibration for the micro-scanning position point (not adaptively calibrating each micro-scanning position). Comparing Fig.13(a) and Fig.13(b), it can be found that the details of the reconstructed image after the adaptive calibration of each point are clearer. Visually, Fig.13(a) appears brighter and has higher spatial resolution

To further prove the effectiveness of the method, we calculated the average of the four reconstructed images' H (as shown in Table 2). It can be seen from the comparison

that the H of the oversampled reconstructed image after adaptive calibration of each point is larger than the H of the zero-point calibration reconstructed image. Combined with the previous simulation experiments, it can be seen that the oversampled reconstructed image with adaptive calibration at each point has higher definition, larger information and richer details, and the spatial resolution is improved compared with the original low-resolution image. The method of adaptive position calibration of each point improves the spatial resolution of the actual system and it is effective.

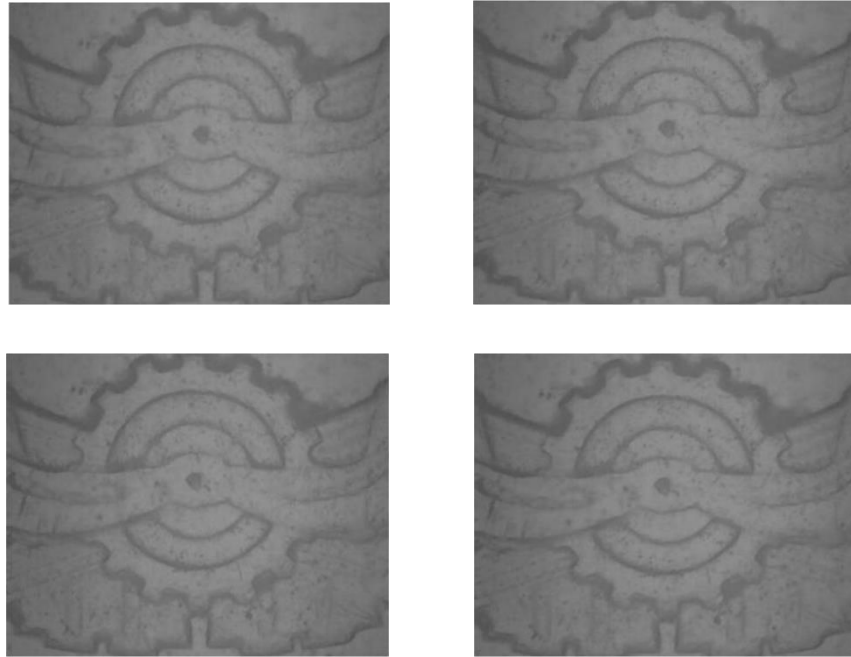
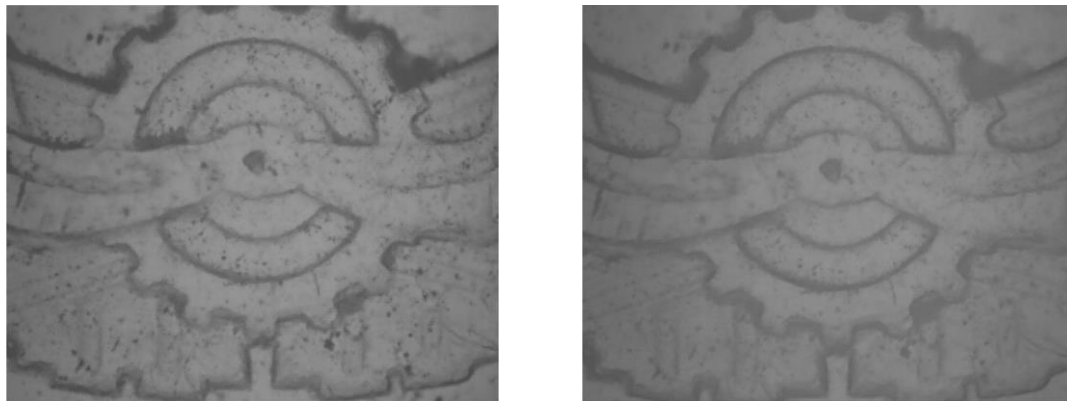


Fig.12 Low-resolution thermal microscope images



(a) Adaptive point calibration

(b) Zero calibration

Fig.13 Reconstruction result of microscopic thermal image oversampling

Table 2 Evaluation scores of thermal microscope images reconstruction experiment

Image processing methods	H
Bilinear interpolation	5.4009
Oversample (no calibration)	5.3869
Oversample(zero calibration)	5.5821
Oversample (adaptive point calibration)	5.7599

5 Conclusion

The introduction of micro-scanning devices in the thermal microscope imaging system enables the system to obtain high-resolution images under limited hardware conditions, which has broad application potential. However, the calibration of the micro-scanning position is a vital part of the practical application of the micro-scanning thermal microscope imaging system. The 2×2 micro-scanning point adaptive position calibration technology proposed in this paper can effectively reduce micro-scanning error and improve the accuracy of the micro-scanning system. Therefore, the adaptive position calibration method can improve the spatial resolution of the micro-scanning thermal microscope imaging system. Due to the simple algorithm and its low complexity, the calibration method proposed in this paper is easy to implement in hardware and enables real-time processing. At the same time, the method can also be applied to other micro-scanning photoelectric imaging systems.

Acknowledgement

This work was supported by NSFC - China (61971373) and Natural Science Foundation of Hebei Province - China (F2019203440) and Science and Technology Support Projects of Key research and Development Plans of Qinhuangdao City - China (201801B010) and Postgraduate innovation ability training funding project of Hebei Provincial Department of Education -China (CXZZSS2019050). The authors gratefully acknowledge funding support from the China Scholarship Council.

References

- [1] Florina Jitescu, Octavian Novac. Staring infrared focal plane arrays for thermal imaging technology[J]. Spie Proceedings, 2000:639-644.
- [2] Christopher D. W. Jones, Cristian A. Bolle, Roland Ryf,等. Opportunities in uncooled infrared imaging: A MEMS perspective[J]. Bell Labs Technical Journal, 2010, 14(3):85-98.
- [3] Zhouzhu Liang. Design and experimental study on micro infrared radiometer chip[J]. Acta optica sinica, 2011, 31(11): 1112009.1-1112009.7.
- [4] Marc P. Hansen, Douglas S. Malchow. Overview of SWIR detectors, cameras, and

- applications[J]. Proceedings of SPIE - The International Society for Optical Engineering, 2008, 6939:69390I-69390I-11.
- [5] Robert J. S. Kyle, Douglas K. van Dover. Uncooled infrared thermal imaging systems for law enforcement[J]. Proceedings of SPIE - The International Society for Optical Engineering, 1995, 2497:98-104.
- [6] G R Ivanitsky, E P Khizhnyak, A A Deev et al. Thermal imaging in medicine: A comparative study of infrared systems operating in wavelength ranges of 3-5 and 8-12 microm as applied to diagnosis[J]. Doklady Biochemistry & Biophysics, 2006, 407(1):59-63.
- [7] Haitao Zhang, Dazun Zhao. Mathematics theory and realization of aliasing reduction in opto-electric imaging system using microscanning[J]. Acta optica sinica, 1999, 19(9): 1263-1268.
- [8] Stephen J. Katzberg, Friedrich O. Huck, Stephen D. Wall. Photosensor Aperture Shaping to Reduce Aliasing in Optical-Mechanical Line-Scan Imaging Systems[J]. Applied Optics, 1973, 12(5):1054-1060.
- [9] Junqi Bai, Qian Chen, Huiming Qu. Research on optical micro scanning reconstruction for infrared starting imaging[J]. J. Infrared and Millimeter Waves, 2008, 27(4): 257-260.
- [10] Fortin J, Chevrette P C. Realization of a fast microscanning device for infrared focal plane arrays[J]. 1996, 2743:185-196.
- [11] Huiming Qu, Qian Chen. Comparison of micro scanning schemes in infrared focal plane array imaging[J]. Laser and Infrared. 2006, 36(3): 161-164.
- [12] Meijing Gao, Weiqi Jin, Xia Wang et al. Design and implementation of optical micro-scanning thermal micro scope imaging system with high resolution[J]. Chinese J. Scientific Instrument. 2009, 30(5): 1037-1041.
- [13] Meijing Gao, Weiqi Jin, Xia Wang et al. Zero calibration for the designed micro scanning thermal microscope imaging system[J]. Acta Optica Sinica, 2009, 29(8):2175-2179.
- [14] Xianmin Wang, Jing Li, Jin Li et al. Multilevel similarity model for high-resolution remote sensing image registration [J]. Infrared Physics and Technology, 2019,505:294-305.
- [15] Meijing Gao. Investigation of high resolution optical micro scanning thermal microscope imaging system[D]. Beijing: Beijing Institute of Technology, 2008,14-67.
- [16] Meijing Gao, Ailing Tan, Bozhi Zhang et al . Design and realization of high resolution optical micro-scanning thermal microscope imaging system[J]. Infrared Physics and Technology, 2018, 95:46-52.
- [17] Meijing Gao, Jie Xu, Ailing Tan et al. Error correction based on micro-scanning preprocessing for an optical micro-scanning thermal microscope imaging system[J]. Infrared Physics and Technology, 2017, 83:252-258.
- [18] Hui Liu, Hailong Shen. Image Match Method Based on Improved SIFT Algorithm[J]. Microelectronics and Computer, 2014, 31(1):38-42.
- [19] Zhou Wang, Alan Conrad Bovik, Hamid Rahim Sheikh et al. Image Quality Assessment: From Error Visibility to Structural Similarity[J]. IEEE Transactions on Image Processing, 2004, 13(4):600-612.

- [20] Jiasu Zheng. An image information entropy-based algorithm of no-reference image quality assessment[D]. Beijing: Beijing Jiaotong University, 2015, 23-25.
- [21] Zhongyuan Guo. Research on infrared image detail enhancement method[D]. Chongqing: Chongqing University of Posts and Telecommunications,2017,41-43.
- [22] Alain Horé, Djemel Ziou. Image quality metrics: PSNR vs. SSIM[C]. Turkey: International Conference on Pattern Recognition, 2010, 2366-2369.